

Field-induced magnetic ordering in $\text{NiCl}_2 \cdot 4\text{SC}(\text{NH}_2)_2$

A. Paduan-Filho,* X. Gratens, and N. F. Oliveira, Jr.

Instituto de Física, Universidade de São Paulo, Caixa Postal 66.318, 05315-970 São Paulo, São Paulo, Brazil

(Received 24 October 2003; published 23 January 2004)

We have investigated the low-temperature T field-induced ordering in $\text{NiCl}_2 \cdot 4\text{SC}(\text{NH}_2)_2$, from magnetization measurements. This is an $S=1$ system with a large single-ion uniaxial anisotropy leaving a singlet ground state. An external magnetic field (\mathbf{B}) parallel to the symmetry axis induces an antiferromagnetically ordered phase for $B_{c1} < B < B_{c2}$. The establishment of this long-range order can be regarded as a Bose-Einstein condensation of magnons. The phase boundaries are predicted to obey power laws $[B_c(T) - B_c(0)] \propto T^\alpha$. The determined phase boundaries could be fitted to power laws yielding $\alpha_1 = 2.63 \pm 0.10$ for $B_{c1}(T)$ and $\alpha_2 = 2.55 \pm 0.10$ for $B_{c2}(T)$.

DOI: 10.1103/PhysRevB.69.020405

PACS number(s): 75.10.Jm, 75.30.Kz

Magnetic systems having a singlet ground state, and with an excitation gap Δ that can be overcome by magnetic fields obtainable in laboratory, have received considerable attention lately,¹⁻⁹ due to the interesting quantum effects exhibited. Antiferromagnetic spin dimers,¹⁻⁶ $S=1$ antiferromagnetic chains,⁷ $S=1/2$ alternating chains,⁸ and even-leg spin ladders⁹ are examples. In these systems, an external magnetic field can lower one of the upper energy levels, which eventually get close to the ground level creating the necessary degeneracy for the appearance of magnetic order. The presence of a small exchange interaction can lead to long-range order (LRO) at a critical field B_{c1} . Further increasing the field should lead to a second transition at B_{c2} after which the system saturates. As pointed out many years ago,¹⁰ the onset of this LRO can be viewed as a Bose-Einstein condensation (BEC) of magnons and recent papers have addressed specifically to this point.¹⁻⁶

The first attempt to interpret this field-induced order in the context of BEC was done by Nikuni *et al.*² Their Hartree-Fock-Popov calculation (HFP-BEC) was able to explain qualitative aspects of the experimental data for the compound TiCuCl_3 (a coupled spin-dimer system) which were in clear disagreement with the predictions of mean-field theory (MFT).^{11,12} One of such aspects is the behavior of the magnetization M as a function of temperature T near B_{c1} where a cusplike dip was observed. Another aspect is the power-law behavior of the observed phase boundary

$$B_c(T) - B_c(0) \propto T^\alpha. \quad (1)$$

Although the BEC picture does predict a power law, in qualitative agreement with the data, the value of α_1 calculated by Nikuni *et al.*² for $B_{c1}(T)$, $\alpha_1 = 1.5$, differed somewhat from the best fit to the TiCuCl_3 data which yielded $\alpha_1 = 2.2$.^{2,5} Subsequent neutron-diffraction studies, confirmed the BEC character of the transition.^{1,6}

To further investigate this point, Wessel *et al.*³ have obtained the entire field-induced phase diagram applying quantum Monte Carlo technique to the three-dimensional (3D) antiferromagnetic spin-1/2 Heisenberg model with spatially anisotropic exchange couplings. Magnetization simulations with Hamiltonians appropriate for weakly coupled dimers (such as TiCuCl_3) and weakly coupled Heisenberg ladders

were made. The general characteristics of the $M(T)$ curve were found to agree qualitatively with the isotropic HFP-BEC. Both phase boundaries, $B_{c1}(T)$ and $B_{c2}(T)$, determined from the extrema in $M(T)$, could be fitted to power laws up to temperatures close to the highest-ordering temperature, for both Hamiltonians. The best exponents for the dimers case were $\alpha_1 = 2.7 \pm 0.2$ and $\alpha_2 = 2.3 \pm 0.2$ for $B_{c1}(T)$ and $B_{c2}(T)$, respectively, and $\alpha_1 = 3.1 \pm 0.2$ and $\alpha_2 = 1.8 \pm 0.2$ for the ladder case. The values of α for B_{c1} , however, are quite different from the isotropic HFP-BEC prediction. So, although at least part of the disagreement could be attributed to the inadequacy of the Hartree-Fock approach in the critical region, it was concluded that the values of the exponents should depend strongly on the dimensionality and quantum dynamics of the particular system.

So far, the focus of the attention has been on low-dimensional systems such as dimers and chains. Field-induced order, however, can also exist in three-dimensional compounds with large single-ion anisotropy, and they also should exhibit BEC.² In an $S=1$ spin system, such as in a Ni^{++} compound, for instance, a cubic crystalline field leaves a spin triplet as the ground state and distortions of the cubic symmetry can lift the degeneracy. An axially symmetric distortion of the proper sign can split the triplet into a lower singlet separated from an excited doublet by an energy $|D|$ (usually D is chosen to be negative in this case). With a singlet ground state, small antiferromagnetic exchange interactions ($2z|J| < |D|$, where z is the number of neighbors) cannot produce LRO. The presence of an external magnetic field parallel to the distortion axis, however, induces LRO between $B_{c1}(T)$ and $B_{c2}(T)$. MFT (Refs. 12 and 13) gives (for isotropic J and $T=0$) $g_{\parallel} \mu_B B_{c1}(0) = |D| - 2z|J| = \Delta$ and $g_{\parallel} \mu_B B_{c2}(0) = |D| + 4z|J|$, where g_{\parallel} is the parallel spectroscopic factor and μ_B is the Bohr magneton. One example of such a system is the compound $\text{NiCl}_2 \cdot 4\text{SC}(\text{NH}_2)_2$, dichlorotetrakis-thiourea-nickel (II), hereon referred to as DTN, for short.¹⁴ In this paper we report magnetization measurements on DTN in fields and temperatures covering the entire ordered phase. $B_{c1}(T)$ and $B_{c2}(T)$ were determined and could be fitted to Eq. (1) yielding values for α_1 and α_2 .

DTN is a tetragonal crystal, space group $I4$, with two molecules in the unit cell. Its magnetic susceptibility up to an external field of 7 K has already been investigated.¹⁴ The

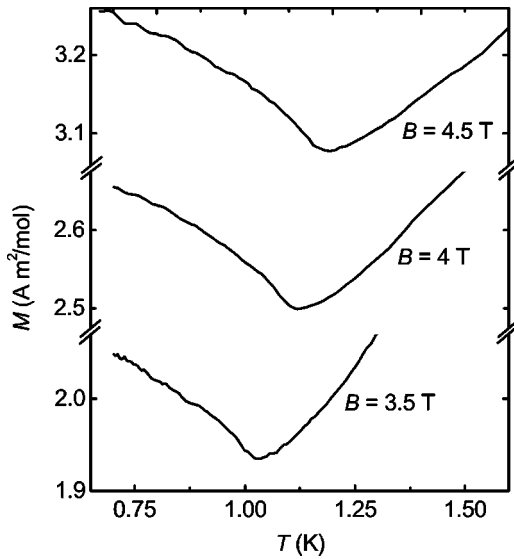


FIG. 1. Magnetization as a function of temperature for three values of field. The onset of the LRO (at low temperature) is marked by a dip, a behavior found in other field-induced LRO compounds investigated (Refs. 2 and 4).

zero-field susceptibility parallel and perpendicular to the tetragonal axis, led to the values $g_{\parallel} = 2.26 \pm 0.03$ and $g_{\perp} = 2.34 \pm 0.03$, and $|D|/k_B = 7.6 \pm 0.4$ K. An isotropic antiferromagnetic interaction J , weaker than D , is also present, and the same data yielded $2z|J|/k_B = 4.5 \pm 0.3$ K. A combination of this interaction with an applied field parallel to the tetragonal axis induces LRO. The spins align antiferromagnetically perpendicular to the field, and part of the B - T phase diagram had already been established.¹⁴

The establishment of similar field-induced LRO in other spin systems, such as dimers and chains, has been interpreted in the context of BEC of magnons. An important constraint is the existence of rotational symmetry around the applied field, to maintain constant the number of magnons. In the present system, the uniaxial symmetry ensures that, making it a quite suitable model system to study BEC.

In the present work magnetization traces were taken up to 17 T with a vibrating sample magnetometer adapted to be used in a ³He cryostat.¹⁵ The DTN single crystals were grown from aqueous solutions of thiourea and nickel chloride. The external field, produced by a superconducting coil, was always carefully aligned with the tetragonal axis of the samples. One difficulty in determining the exponent α from the phase boundaries comes from the fact that Eq. (1) has to be fitted to the data varying both α and $B_c(0)$ and the value of α turns out to be quite sensitive to $B_c(0)$. In order to minimize this problem we have measured the magnetization at the temperature of $T = 0.016$ K up to 17 T with a force magnetometer¹⁶ and inside a plastic dilution refrigerator.¹⁷ This practically determined $B_{c1}(0)$ and $B_{c2}(0)$ with the accuracy of the force magnetometer, which was comparable to that of the vibrating sample magnetometer.

Initially we have measured M as a function of T at constant B . Figure 1 shows traces for three different fields, near B_{c1} . The transition to the ordered state is marked by a dip in

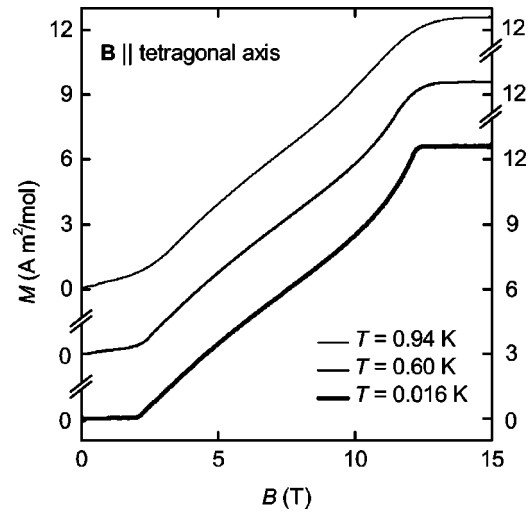


FIG. 2. Magnetization traces for three different temperatures. The $T = 0.016$ K trace is representative of the $T = 0$ magnetization.

$M(T)$, similar to what was found in the low-dimensional compounds^{2,4} and different from the prediction of MFT. The phase boundaries, however, were actually obtained from traces of M versus B at constant T . We believe this method to be more accurate, especially at low temperatures where the boundary is quite flat.

Figure 2 shows three magnetization traces for the temperatures $T = 0.016$ K, $T = 0.60$ K, and $T = 0.94$ K, with \mathbf{B} parallel to the tetragonal axis, and Fig. 3 shows their numerical derivatives dM/dB . The $T = 0.016$ K trace shows following sharp features: (i) M is zero up to very close to $B_{c1} = 2.105 \pm 0.010$ T which is marked by a sharp change in dM/dB ; (ii) at this point antiferromagnetic LRO is established with the spins perpendicular to \mathbf{B} ,¹² and dM/dB changes to the value 1.26 A m²/(mol T); (iii) this susceptibility, which is initially independent of the field, first decreases and then increases going to a λ -like peak at B_{c2}

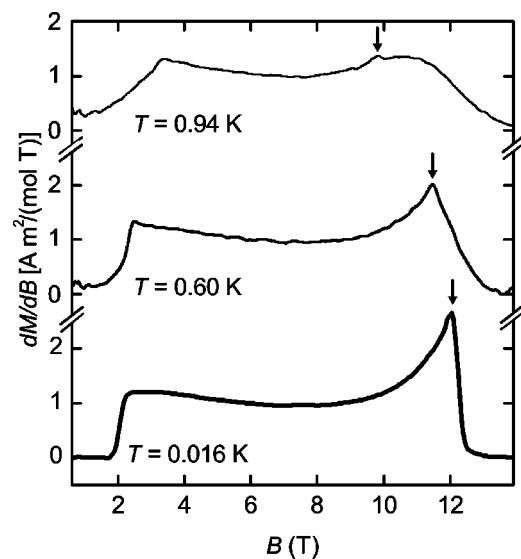


FIG. 3. Differential magnetizations numerically obtained for the traces in Fig. 2.

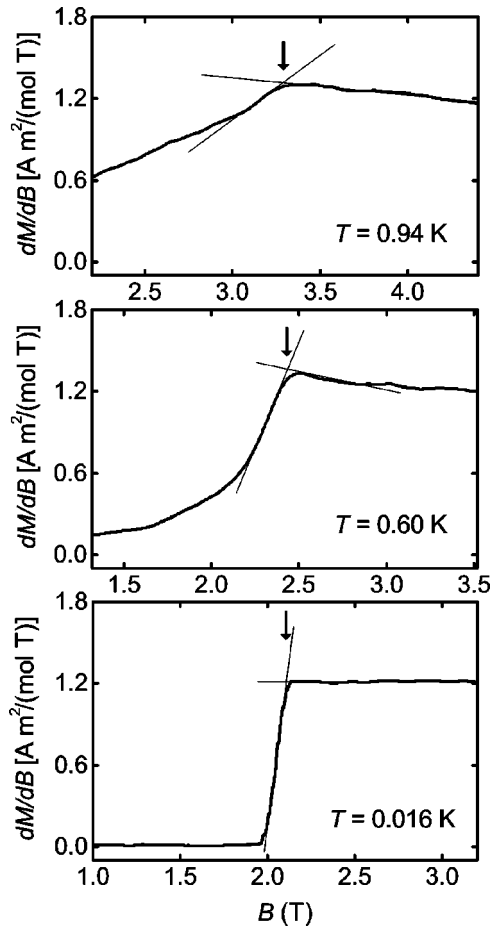


FIG. 4. Detail of the B_{c1} region for the traces in Fig. 3. B_{c1} was taken at the edge obtained from extrapolations, varying the numbers of points used for the derivation process (see text).

$=12.11 \pm 0.03$ T; (iv) immediately after B_{c2} , M reaches the saturation value $M_s = 12.6 \pm 0.2$ A m²/mol (the error is mostly due to the calibration of the magnetometer).

The measured value of M_s agrees quite well with $N_0 g_{\parallel} \mu_B S = 12.62 \pm 0.17$ A m²/mol, taking $g_{\parallel} = 2.26 \pm 0.03$ from Ref. 14 and $S = 1$. Assuming the values of B_{c1} and B_{c2} , taken from the curves for $T = 0.016$ K, as the $T = 0$ values, the MFT relations give $|D|/k_B = 8.26 \pm 0.10$ K and $2|J|z/k_B = 5.06 \pm 0.10$ K. These values are about 10% higher than the ones obtained from zero-field susceptibility fits in Ref. 14. It is interesting to note that the measured value of dM/dB just above B_{c1} , at $T = 0.016$ K, is equal to $M_s/(B_{c2} - B_{c1})$ the MFT prediction for $T = 0$.¹² Also interesting is the continuity of M at B_{c1} . This confirms the disordered character of the spin system below B_{c1} as a consequence of the singlet ground state, as concluded in Ref. 14. A doublet ground state would have produced antiferromagnetic LRO at $B = 0$, with the spins parallel to the easy axis, and the transition at B_{c1} should show a magnetization jump $\Delta M \cong [M_s/(B_{c2} - B_{c1})]B_{c1} \cong 2.5$ A m²/mol (spin-flop transition). A discontinuity of this magnitude could not be missed in our data.

The values of $B_{c1}(T)$ and $B_{c2}(T)$ were obtained from

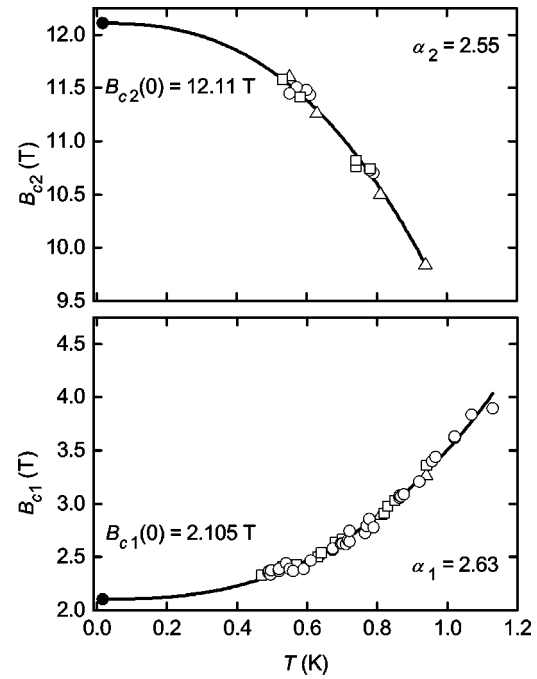


FIG. 5. Lower and upper phase boundaries as determined from magnetization traces. Different symbols refer to independent runs.

numerical differentiation of the M data. Figure 4 shows three examples of the determination of $B_{c1}(T)$. The differentiation was done by the usual technique of choosing, at each M data point, a number of experimental points before and after, and making a polynomial fit. Since this introduces artificial rounding in dM/dB , the extrapolations shown were made considering several dM/dB traces made with different number of M points. As can be seen in Fig. 3, at the lowest temperatures, B_{c2} is marked by a λ -like peak. At higher temperatures a bulge develops above the B_{c2} peak, and at the highest temperatures the λ peak has faded into just a cusp before a broad rounded maximum. The value of B_{c2} was always taken at the peak. The determined values of $B_{c1}(T)$ and $B_{c2}(T)$ were then fitted to Eq. (1) yielding $\alpha_1 = 2.63 \pm 0.10$ for $B_{c1}(T)$ and $\alpha_2 = 2.55 \pm 0.10$ for $B_{c2}(T)$. Figure 5 shows the data and best fits. The uncertainty quoted corresponds to twice the standard deviation for the fit to all the points. The experimental points were obtained in three independent runs. Separate fits to each run were also made and the resulting values of α and standard deviations were always inside the quoted interval. We have also estimated the demagnetization corrections, which were small enough not to have any significant effect in α . The values of α here obtained are near but definitely different from those obtained for low-dimensional dimers and chains, from theory or experiment. It is interesting to note that the exponents for both boundaries $B_{c1}(T)$ and $B_{c2}(T)$ do not differ by more than the quoted uncertainty.

In conclusion, we have determined the field-induced phase transitions for $\text{NiCl}_2 \cdot 4\text{SC}(\text{NH}_2)_2$, a $S = 1$ system, with a singlet ground state due to a single-ion uniaxial anisotropy larger than the isotropic exchange. This field-

induced ordering transition has been interpreted recently in systems of different symmetry as a manifestation of BEC of magnons. The phase boundaries at low and high fields could be fitted to power laws yielding, respectively, the exponents $\alpha_1 = 2.63 \pm 0.10$ and $\alpha_2 = 2.55 \pm 0.10$. We hope that the present data will stimulate theoretical work appropriate for this system.

The authors are indebted to V. Bindilatti and Y. Shapira for enlightening discussions. This research was supported by FAPESP (Fundação de Amparo à Pesquisa do Estado de São Paulo, Brazil) under Contract No. 99/10359–7. Two of the authors, A.P.F. and N.F.O.J., acknowledge support from CNPq (Conselho Nacional de Desenvolvimento Científico e Tecnológico, Brazil).

*Electronic address: apaduan@if.usp.br

- ¹C. Rugg, N. Cavadini, A. Furrer, H.-U. Gudel, K. Kramer, H. Mutka, A. Wildes, K. Habicht, and P. Vorderwisch, *Nature* (London) **423**, 62 (2003).
- ²T. Nikuni, M. Oshikawa, A. Oosawa, and H. Tanaka, *Phys. Rev. Lett.* **84**, 5868 (2000).
- ³S. Wessel, M. Olshanii, and S. Haas, *Phys. Rev. Lett.* **87**, 206407 (2001).
- ⁴A. Oosawa, T. Takamasu, K. Tatani, H. Abe, N. Tsujii, O. Suzuki, H. Tanaka, G. Kido, and K. Kindo, *Phys. Rev. B* **66**, 104405 (2002).
- ⁵A. Oosawa, H. Aruga-Katori, and H. Tanaka, *Phys. Rev. B* **63**, 134416 (2001).
- ⁶H. Tanaka, A. Oosawa, T. Kato, H. Uekusa, Y. Ohashi, K. Kakurai, and A. Hoser, *J. Phys. Soc. Jpn.* **70**, 939 (2001).
- ⁷Y. Ajiro, T. Goto, H. Kikuchi, T. Sakakibara, and T. Inami, *Phys. Rev. Lett.* **63**, 1424 (1989).
- ⁸D.A. Tennant, C. Broholm, D.H. Reich, S.E. Nagler, G.E. Granroth, T. Barnes, K. Damle, G. Xu, Y. Chen, and B.C. Sales, *Phys. Rev. B* **67**, 054414 (2003).
- ⁹H. Mayaffre, M. Horvatic, C. Berthier, M.-H. Julien, P. Ség-ransan, L. Lévy, and O. Piovesana, *Phys. Rev. Lett.* **85**, 4795 (2000).
- ¹⁰I. Affleck, *Phys. Rev. B* **43**, 3215 (1991); T. Matsubara and H. Matsuda, *ibid.* **16**, 569 (1956).
- ¹¹M. Tachiki and T. Yamada, *J. Phys. Soc. Jpn.* **28**, 1413 (1970).
- ¹²T. Tsuneto and T. Murao, *Physica* (Amsterdam) **51**, 186 (1971).
- ¹³K.M. Diederix, J.P. Groen, T.O. Klaassen, N.J. Poulis, and R.L. Carlin, *Physica B* **97**, 113 (1979).
- ¹⁴A. Paduan-Filho, R.D. Chirico, K.O. Joung, and R.L. Carlin, *J. Comput. Phys.* **74**, 4103 (1981).
- ¹⁵N.F. Oliveira, Jr. and S. Foner, *Rev. Sci. Instrum.* **43**, 37 (1972).
- ¹⁶V. Bindilatti and N.F. Oliveira, Jr., *Physica B* **194**, 63 (1994).
- ¹⁷E. ter Haar, R. Wagner, C.M.C.M. van Woerkens, S.C. Steel, G. Frossati, L. Skrbek, M.W. Meisel, V. Bindilatti, A.R. Rodrigues, R.V. Martin, and N.F. Oliveira, Jr., *J. Low Temp. Phys.* **99**, 151 (1995).